

when present, can occur in this gap and partly fill it so that such experiments could provide another check of the present theory.

Another case where fast-electron energy losses were observed is x-ray photoemission,<sup>18</sup> where the electron created in the solid can excite both bulk and surface plasmons. The extension of our theory to this case could be worked out,<sup>15</sup> though the situation here is more complicated by the presence of the hole. Its lifetime and the relaxation of the Fermi sea via low-energy electron-hole pair excitations modify the shape of the emitted-electron spectral lines.<sup>19</sup> These effects could be treated in-

dependently of the discrete plasmon losses, but in thin films they might interfere with the surface plasmon emission from the region of strong dispersion.

#### ACKNOWLEDGMENTS

The authors would like to thank Professor Abdus Salam, the International Atomic Energy Agency, and UNESCO for hospitality at the International Centre for Theoretical Physics, Trieste. They are also grateful to Professor S. Lundqvist for critical reading of the manuscript and Dr. R. Guardiola for help with numerical analysis.

\*Permanent address: Institute Rudjer Bošković, Zagreb, Yugoslavia.

†Chargé de Recherches au Fonds National Belge de la Recherche Scientifique. Present address: European Space Research Organization, Noordwyk, Holland.

<sup>1</sup>See, e.g., D. Pines, *Elementary Excitations in Solids* (Benjamin, New York, 1964).

<sup>2</sup>For further references see, H. Raether, *Springer Tracts in Modern Physics* (Springer, Berlin, 1965), Vol. 38, p. 84.

<sup>3</sup>J. Geiger and K. Wittmaack, *Z. Physik* **195**, 44 (1966).

<sup>4</sup>A. A. Lucas, E. Kartheuser, and R. Badro, *Solid State Commun.* **8**, 1075 (1970); *Phys. Rev.* (to be published).

<sup>5</sup>In the LEED case, however, the recoil of the electron in the plasmon emission cannot be neglected.

<sup>6</sup>J. B. Chase and K. L. Kliewer, *Phys. Rev.* (to be published). We thank the authors for sending us the preprint of this work prior to publication.

<sup>7</sup>M. Šunjić, A. A. Lucas, and M. Tomaš (unpublished).

<sup>8</sup>The application of the theory to the electron-phonon coupling is straightforward.

<sup>9</sup>R. Fuchs and K. L. Kliewer, *Phys. Rev.* **140**, 2076 (1965).

<sup>10</sup>M. Born and K. Huang, *Dynamical Theory of*

*Crystal Lattices* (Clarendon, Oxford, England, 1966).

<sup>11</sup>The S polarization eigenmodes do not couple to the electron.

<sup>12</sup>The present derivation of the dielectric properties of the free-electron gas from those of an ionic plasma is similar to a recent study where the Wigner electron lattice is described as a limiting case of the classical Lorentz lattice, see A. Bagchi, *Phys. Rev.* **178**, 707 (1969).

<sup>13</sup>E. N. Economou, *Phys. Rev.* **182**, 539 (1969).

<sup>14</sup>A treatment formally similar to ours has been recently applied, e.g., in the x-ray problem, by K. D. Schotte and U. Schotte, *Phys. Rev.* **182**, 479 (1969), to the singular electron-hole pair scattering, and by D. C. Langreth, *Phys. Rev. B* **1**, 471 (1970) to the deep hole screening by plasmons in the uniform electron gas.

<sup>15</sup>M. Šunjić and A. A. Lucas (unpublished).

<sup>16</sup>C. J. Powell, *Phys. Rev.* **175**, 972 (1968).

<sup>17</sup>H. Ibach, *Phys. Rev. Letters* **24**, 1416 (1970).

<sup>18</sup>See, e.g., S. Hagström, C. Nordling, and K. Siegbahn, in *Alpha-, Beta- and Gamma-Ray Spectroscopy*, edited by K. Siegbahn (North-Holland, Amsterdam, 1965), p. 845.

<sup>19</sup>S. Doniach and M. Šunjić, *J. Phys. C* **3**, 285 (1970).

## Analysis of the Magnetic Susceptibility of $K_2OsCl_6$

H. U. Rahman

*Department of Mathematics, Heriot-Watt University, Edinburgh, United Kingdom*

(Received 1 July 1970)

The configuration interaction between the  $t_{2g}^4$  and  $t_{2g}^3e$  configurations has been taken into account to calculate the energy levels of the  $(OsCl_6)^{2-}$  complex ion in the intermediate-coupling scheme. The matrix elements of the magnetic moment operator between the ground level  $A_1$  and the excited  $T_1$  levels are given in algebraic form, and then used to calculate the temperature-independent paramagnetic susceptibility. The experimental value of the susceptibility and a part of the optical absorption spectrum can be fitted to theory by choosing the following values of the parameters:  $B = 365.5 \text{ cm}^{-1}$ ,  $C = 1561.0 \text{ cm}^{-1}$ ,  $\xi_{5d} = 2575.0 \text{ cm}^{-1}$ ,  $\Delta = 33\,000.0 \text{ cm}^{-1}$ ,  $k = 0.7$ ,  $k' = 0.7$ .

### I. INTRODUCTION

In complexes of the type  $X_2YZ_6$ , where X is an

alkali ion [(or  $NH_4$ ,  $C(NH_3)_4$ , etc.)], Y is a metal ion of the 4d or 5d group, and Z is a halogen ion, unlike the corresponding complexes of the iron

group, the spin-orbit interaction is large and comparable in magnitude with the electrostatic interaction. Therefore, the spin-orbit interaction cannot be treated as a first-order perturbation to analyze the optical absorption spectra of the complexes. Further, the Kotani theory,<sup>1</sup> which assumed  $\zeta_{nd}$  to be small and which was successful in the iron-group complexes, cannot be applied to explain their magnetic properties. The large value of the spin-orbit constant also makes it desirable to take into account the configuration interaction. A number of authors<sup>2-5</sup> have done such complete calculations by simultaneously diagonalizing the crystal-field, electrostatic, and spin-orbit interactions for the octahedrally coordinated compounds where the central ion has two or three  $d$  electrons outside the closed shell. Schroeder<sup>6</sup> has done intermediate-coupling calculations to interpret the optical spectrum of  $K_2IrCl_6$ .

In this paper, we are interested in the analysis of the absorption spectrum and magnetic susceptibility of  $K_2OsCl_6$ . According to Wyckoff,<sup>7</sup> the structure of  $(OsCl_6)^{2-}$  is such that the osmium ion ( $5d^4$ ) is surrounded by six chlorine ions placed at the corners of an octahedron. We shall use this model for our purpose. Jørgensen<sup>8-10</sup> has given the absorption spectrum of  $K_2OsCl_6$ , and the experimental value of the magnetic susceptibility has also been reported.<sup>11-14</sup>

## II. CALCULATION OF ENERGY LEVELS

In a strong octahedral field, the  $d$  shell is split into a threefold subshell and a twofold subshell, labeled by the irreducible representations  $t_2$  and  $e$  of the octahedral group. Strong-field states are constructed from the configuration  $t_2^n e^m$  ( $n \leq 6$ ,  $m \leq 4$ ). The terms  $S_1\Gamma_1$  of the  $t_2^n$  configuration, which are allowed by the exclusion principle, are coupled with the allowed terms  $S_2\Gamma_2$  of  $e^m$  to give the resultant terms  $S\Gamma$ . The terms arising from the  $t_2^4$  and  $t_2^3e$  configurations are as follows:

$$t_2^4: {}^3T_1, {}^1E, {}^1T_2, {}^1A_1$$

$$t_2^3e: {}^5E, {}^3A_1, {}^3A_2, {}^2^3E, {}^2^3T_1, {}^2^3T_2, {}^1A_1,$$

$${}^1A_2, {}^1E, {}^2^1T_1, {}^2^1T_2.$$

When the spin-orbit interaction is comparable with the electrostatic energy, the appropriate coupling scheme is  $|t_2^n(S_1\Gamma_1)e^m(S_2\Gamma_2)S\Gamma t\rangle$ . (This is analogous to the  $|\alpha SLJ\rangle$  scheme in atomic spectroscopy).  $S=0$  corresponds to the irreducible representation  $A_1$  and  $S=1$  corresponds to  $T_1$ , etc. The spin  $S$  and space functions  $\Gamma$  are coupled to form bases for irreducible representations of the octahedral group. The spin-orbit interaction splits the  $S\Gamma$  terms into  $t$  levels, e. g.,  ${}^3T_1$  is split into  $A_1$ ,  $E$ ,  $T_1$ , and  $T_2$  (because  $T_1 \times T_1 = A_1 + E + T_1 + T_2$ ). The spin-orbit interaction matrices, in this scheme,

are  $6 \times 6$ ,  $8 \times 8$ ,  $11 \times 11$ , and  $12 \times 12$  for  $A_1$ ,  $E$ ,  $T_1$ , and  $T_2$  levels, respectively, which were taken from Schroeder.<sup>6</sup> The  $A_2$  levels, which come from the  $t_2^3e$  configuration, were ignored because they do not contribute to the magnetic susceptibility (see Sec. III). These matrices were combined with the corresponding matrices of electrostatic interaction, and the crystal-field parameter  $\Delta (= 10Dq)$  was added in the diagonal interaction elements of the states arising from the  $t_2^3e$  configuration.

The absorption spectrum of  $K_2OsCl_6$  has been measured by Jørgensen,<sup>8-10</sup> and by far the best established level is the one at  $17240 \text{ cm}^{-1}$ , being the  $t_2^4 {}^1A_1A_1$  level. The two broad bands at  $10800$  and  $11700 \text{ cm}^{-1}$  represent both  $E$  and  $T_2$  components of  $t_2^4 {}^1E$  and  $t_2^4 {}^1T_2$ . The combined interaction matrices were diagonalized on a fast computer for various values of the spin-orbit parameter  $\zeta_{5d}$ , Racah parameters  $B$  and  $C$ , and the crystal-field

TABLE I. Calculated energy levels of  $K_2OsCl_6$ .

Level	Energy ( $\text{cm}^{-1}$ )	Dependence on			
		$\delta B$	$\delta C$	$\delta \zeta_{5d}$	$\delta \Delta$
$A_1$	0				
$T_1$	2 649.95	-0.0205	-0.3278	1.4326	-0.0157
$T_2$	4 461.99	0.4552	0.0886	1.8286	-0.0167
$E$	4 587.02	0.7985	-0.0212	1.9044	-0.0174
$T_2$	9 861.77	3.1688	1.3094	2.7753	-0.0147
$E$	10 110.79	4.7558	1.3801	2.6758	-0.0203
$A_1$	17 222.46	8.4160	4.0759	2.8224	0.0156
$T_2$	27 617.38	-5.0983	-5.0258	2.3456	0.9480
$E$	27 700.33	-5.0174	-4.9571	2.3804	0.9436
$T_1$	27 872.83	-4.9200	-4.9270	2.4893	0.9379
$A_1$	28 182.85	-5.0290	-5.0105	2.8042	0.9279
$T_1$	34 327.67	0.1210	-0.6971	1.5304	0.9524
$T_1$	35 412.42	-0.4186	-0.9455	2.1829	0.9521
$A_1$	35 432.87	-0.8167	-0.8529	2.4172	0.9345
$T_2$	35 833.56	0.0559	-1.1388	2.4038	0.9515
$E$	36 465.72	0.7775	-0.7644	2.5241	0.9356
$T_1$	36 861.06	0.3634	-1.0591	2.7256	0.9503
$T_2$	37 099.39	2.9305	-0.5956	2.1782	0.9499
$E$	37 387.73	0.2594	-1.0048	2.9991	0.9435
$T_2$	37 495.51	0.9279	-1.0446	2.9904	0.9419
$T_1$	37 667.45	3.2668	-1.2439	2.7681	0.9481
$T_2$	38 381.32	6.9480	-1.0636	2.3643	0.9519
$T_1$	39 234.36	8.1616	-1.2479	2.6486	0.9508
$T_2$	39 327.94	7.7159	-1.1623	2.8845	0.9362
$T_2$	40 808.66	5.8196	0.3449	2.6512	0.9489
$T_1$	42 112.25	6.4119	0.8885	2.7446	0.9489
$E$	42 289.43	10.8563	0.5371	2.3889	0.9494
$E$	45 015.70	16.9193	0.4934	2.6311	0.9481
$T_2$	45 128.93	15.1172	0.4284	3.0130	0.9446
$T_2$	45 420.63	12.6731	0.5407	3.3272	0.9510
$T_1$	45 897.27	17.4136	0.5234	2.8569	0.9503
$A_1$	46 268.35	23.3707	0.9358	2.6655	0.8910
$T_1$	46 801.60	14.8375	0.4998	3.5728	0.9515
$E$	47 222.29	14.9445	0.3086	4.0049	0.9384
$A_1$	48 218.81	16.5294	0.3304	4.0472	0.9467
$T_1$	50 053.70	19.3126	1.7476	3.4354	0.9522
$T_2$	51 756.96	24.2270	2.2762	3.2510	0.9387

TABLE II. Compositions of the levels of  $t_2^4$  configuration and the first two  $T_1$  levels of  $t_2^3e$  configuration.

Level	Energy (cm <sup>-1</sup> )	Composition
$t_2^3T_1A_1$	0	$0.94216t_2^3T_1 - 0.25484t_2^4A_1 - 0.13406t_2^3(A_2)e^5E$ $- 0.07375t_2^3(^2T_1)e^3T_1 + 0.12307t_2^3(^2T_2)e^3T_1$ $- 0.09402t_2^3(^2E)e^1A_1$
$t_2^3T_1T_1$	2649.95	$- 0.98404t_2^3T_1 - 0.12617t_2^3(A_2)e^5E - 0.05771t_2^3(^2E)e^3A_1$ $- 0.02807t_2^3(A_2)e^3E + 0.02705t_2^3(^2E)e^3E$ $+ 0.02590t_2^3(^2T_1)e^3T_1 - 0.06264t_2^3(^2T_2)e^3T_1$ $+ 0.02759t_2^3(^2T_1)e^3T_2 + 0.03879t_2^3(^2T_2)e^3T_2$ $- 0.05419t_2^3(^2T_1)e^1T_1 + 0.03299t_2^3(^2T_2)e^1T_1$
$t_2^3T_1T_2$	4461.99	$0.88849t_2^3T_1 - 0.42414t_2^4T_2 + 0.06782t_2^3(A_2)e^5E$ $- 0.03465t_2^3(^2E)e^3A_2 - 0.04056t_2^3(A_2)e^3E + 0.07619$ $t_2^3(^2E)e^3E + 0.09667t_2^3(^2T_1)e^3T_1 - 0.00565t_2^3(^2T_2)e^3T_1$ $- 0.00425t_2^3(^2T_1)e^3T_2 - 0.00767t_2^3(^2T_2)e^3T_2 - 0.01999$ $t_2^3(^2T_1)e^1T_2 - 0.08704t_2^3(^2T_2)e^1T_2$
$t_2^3T_1E$	4587.02	$- 0.90909t_2^3T_1 + 0.37894t_2^4E - 0.09787t_2^3(A_2)e^5E$ $- 0.06288t_2^3(^2T_1)e^3T_1 - 0.03874t_2^3(^2T_2)e^3T_1 - 0.09919$ $t_2^3(^2T_1)e^3T_2 - 0.06823t_2^3(^2T_2)e^3T_2 + 0.02058t_2^3(^2E)e^1E$
$t_2^4T_2T_2$	9861.77	$0.43435t_2^4T_1 + 0.88241t_2^4T_2 + 0.03788t_2^3(A_2)e^5E$ $+ 0.07713t_2^3(^2E)e^3A_2 - 0.03354t_2^3(A_2)e^3E - 0.05125$ $t_2^3(^2E)e^3E - 0.03954t_2^3(^2T_1)e^3T_1 + 0.04621t_2^3(^2T_2)e^3T_1$ $- 0.06182t_2^3(^2T_1)e^3T_2 - 0.07395t_2^3(^2T_2)e^3T_2 - 0.05047$ $t_2^3(^2T_1)e^1T_2 + 0.07756t_2^3(^2T_2)e^1T_2$
$t_2^4EE$	10110.79	$- 0.38357t_2^4T_1 - 0.90873t_2^4E - 0.04880t_2^3(A_2)e^5E$ $- 0.03784t_2^3(^2T_1)e^3T_1 + 0.05473t_2^3(^2T_2)e^3T_1 + 0.11753$ $t_2^3(^2T_1)e^3T_2 - 0.00940t_2^3(^2T_2)e^3T_2 + 0.07978t_2^3(^2E)e^1E$
$t_2^4A_1A_1$	17222.46	$0.28170t_2^3T_1 + 0.92603t_2^4A_1 - 0.05903t_2^3(A_2)e^5E$ $+ 0.00898t_2^3(^2T_1)e^3T_1 - 0.15229t_2^3(^2T_2)e^3T_1$ $+ 0.19064t_2^3(^2E)e^1A_1$
$t_2^3(A_2)e^5ET_1$	27872.83	$0.12139t_2^3T_1 - 0.96949t_2^3(A_2)e^5E + 0.05046$ $t_2^3(^2E)e^3A_1 + 0.00798t_2^3(A_2)e^3E - 0.03386t_2^3(^2E)e^3E$ $+ 0.04813t_2^3(^2T_1)e^3T_1 - 0.14228t_2^3(^2T_2)e^3T_1 - 0.06304$ $t_2^3(^2T_1)e^3T_2 - 0.11433t_2^3(^2T_2)e^3T_2 + 0.04087$ $t_2^3(^2T_1)e^1T_1 - 0.01767t_2^3(^2T_2)e^1T_1$
$t_2^3(A_2)e^3ET_1$	34327.67	$0.01452t_2^3T_1 + 0.01318t_2^3(A_2)e^5E + 0.20170$ $t_2^3(^2E)e^3A_1 + 0.56662t_2^3(A_2)e^3E + 0.33150t_2^3(^2E)e^3E$ $+ 0.45008t_2^3(^2T_1)e^3T_1 - 0.23747t_2^3(^2T_2)e^3T_1$ $+ 0.32478t_2^3(^2T_1)e^3T_2 + 0.31052t_2^3(^2T_2)e^3T_2 + 0.09292$ $t_2^3(^2T_1)e^1T_1 - 0.24183t_2^3(^2T_2)e^1T_1$

TABLE III. Matrix elements of  $(L_z + 2S_z)$  between the  $A_1$  and  $T_1$  states.

$T_1$	$t_2^3(T_1)e^{-1}T_1$	$t_2^3(T_2)e^{-1}T_1$	$t_2^3(T_2)e^{-1}T_1$	$t_2^3(T_1)e^{-1}T_1$	$t_2^3(E)e^{-1}A_1$	$t_2^3(A_2)e^{-1}E$	$t_2^3(E)e^{-1}E$	$t_2^3(T_1)e^{-1}T_1$	$t_2^3(T_2)e^{-1}T_1$	$t_2^3(T_1)e^{-1}T_2$	$t_2^3(T_2)e^{-1}T_2$	$t_2^3(A_2)e^{-1}E$
$t_2^3(A_1)$	0	$4/\sqrt{3}ik'$	0	0	0	0	0	0	0	0	0	0
$t_2^3(E)e^{-1}A_1$	$-\sqrt{2}ik$	0	0	0	0	0	0	0	0	0	0	0
$t_2^3(T_1)$	0	$(2k+4)/\sqrt{6}i$	$2/3ik'$	$4/3ik'$	$2/3ik'$	$2/\sqrt{6}ik'$	$2/3ik'$	$-1/\sqrt{3}ik'$	$1/\sqrt{3}ik'$	$ik'$	$ik'$	0
$t_2^3(T_1)e^{-1}T_1$	0	0	$-ik'$	0	$-2/\sqrt{6}ik$	0	0	0	$1/\sqrt{2}ik$	0	0	0
$t_2^3(T_2)e^{-1}T_1$	0	0	$1/\sqrt{3}ik'$	0	0	0	0	$(k+4)/\sqrt{6}i$	0	0	$-1/\sqrt{2}ik$	0
$t_2^3(A_2)e^{-1}E$	0	0	0	0	0	0	0	0	0	0	0	$2/\sqrt{2}$

parameter  $\Delta$ . The calculations were done in a self-consistent way in the sense that the energy levels were calculated to fit with the experimental spectrum and then the magnetic susceptibility (see Sec. III) was calculated with the same values of the parameters to see how close the agreement was. If the agreement between the calculated and experimental value of the susceptibility was not satisfactory, the parameters were changed slightly and the whole procedure was repeated. In this way, the following values of the parameters were obtained (all in units of  $\text{cm}^{-1}$ ):

$$B = 365.5, \quad C = 1561.0, \tag{1}$$

$$\zeta_{5d} = 2575.0, \quad \Delta = 33\,000.0.$$

The calculated energy levels are given in Table I, which also gives approximate dependence of the energy levels on small changes in  $B$ ,  $C$ ,  $\zeta_{5d}$ , and  $\Delta$  from the above values. The levels arising from the  $t_2^3e$  configuration depend most heavily on the value of  $\Delta$ , and also the dependence is nearly the same for all the levels. Therefore, a change in  $\Delta$  will produce a nearly uniform shift in all these levels. Table I can also be used to calculate energy levels of other  $d^4$  complexes of octahedral symmetry, such as  $(\text{OsBr}_6)^{2-}$ , etc. Table II gives the composition of the levels of the  $t_2^4$  configuration and the first two  $T_1$  levels of the  $t_2^3e$  configuration. The contributions of  $t_2^4\ ^3T_1T_1$ ,  $t_2^3(^4A_2)e^{-1}E$ , and  $t_2^3(^4A_2)e^{-1}E$  levels to the susceptibility are 95.0%, 0.4%, and 4.3%, respectively. All the other  $T_1$  levels make a total contribution of 0.3%.

The low-lying levels belonging to the  $t_2^4$  configuration are not very dependent on  $\Delta$ . To reduce the number of parameters, we kept  $\Delta = 33\,000\ \text{cm}^{-1}$  and made the assumption  $C/B = 4.3$ . In this approximation, the levels of the  $t_2^4$  configuration are shown, in Fig. 1, as functions of  $\zeta_{nd}/B$ .

### III. SUSCEPTIBILITY

The temperature-independent paramagnetic susceptibility  $\chi$  is given by<sup>15</sup>

$$\chi = \left(\frac{2}{3}N\beta^2 \sum_n |\langle \Psi_n | \vec{L} + 2\vec{S} | \Psi_0 \rangle|^2 / (E_n - E_0)\right), \tag{2}$$

where  $N$  is Avogadro's number,  $\beta$  is the Bohr magneton, and the summation is over all the excited states. Both  $\vec{L}$  and  $\vec{S}$  transform as the irreducible representation  $T_1$ . For the  $d^4$  configuration, the lowest term is  $t_2^4\ ^3T_1$  giving  $A_1$  as the ground level, and, therefore, only those levels which transform as  $T_1$  will have nonzero matrix elements with the ground level through the magnetic-moment operator (because  $A_1 \times T_1 = T_1$ ). When the magnetic field is taken along the  $z$  axis and  $E_n - E_0$  is expressed in units of  $\text{cm}^{-1}$ , Eq. (2) can be written as

$$\chi = 0.5106 \sum_n |\langle \Psi_n | (L_z + 2S_z) | \Psi_0 \rangle|^2 / (E_n - E_0). \tag{3}$$

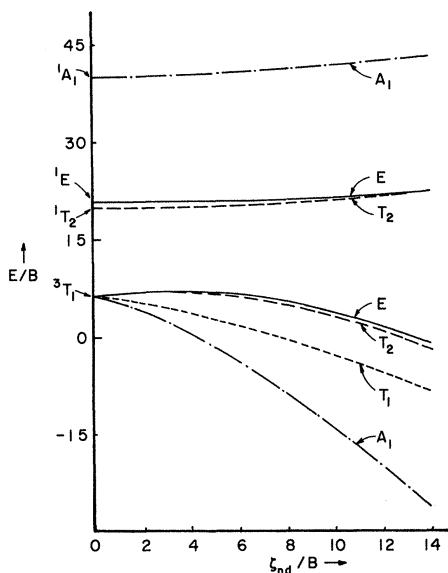


FIG. 1. Energy-level diagram for the  $t_2^4$  configuration.

We also note that  $\vec{L}$  is a one-electron operator and therefore it can connect only those levels which belong to the configurations which differ at the most in one electron (e. g., levels belonging to  $t_2^n$  and  $t_2^{n-1}e$  but not  $t_2^n$  and  $t_2^{n-2}e^2$ ). Further,  $\vec{S}$  is also a one-electron operator, but it can have interaction only within a configuration because of the orthogonality of spatial functions belonging to different configurations.

The compositions of  $\Psi_0$  and  $\Psi_n$  are already known from the analysis of the absorption spectrum. If we calculate the matrix elements of the magnetic-moment operator between the ground level  $A_1$  and the excited levels  $T_1$ , we can calculate the susceptibility from Eq. (3). Tensor-operator methods<sup>16</sup> were used to calculate the matrix elements of the magnetic-moment operator, and they are given in Table III. The matrix elements of  $L_x$  are multiplied by the orbital reduction factors  $k$  and  $k'$ , defined in terms of the one-electron orbital-angular-momentum operator  $\vec{l}$  as

$$\langle t_2 \| \vec{l} \| t_2 \rangle = \sqrt{6}ik,$$

$$\langle t_2 \| \vec{l} \| e \rangle = -2\sqrt{3}ik'.$$

$k$  and  $k'$  are generally less than unity, and  $k$  is not

TABLE IV. Calculated susceptibility for a few values of the orbital reduction factors.

$k$	$k'$	$10^6\chi$
1.0	1.0	1190
0.8	0.8	1007
0.8	0.7	987
0.7	0.8	942
0.7	0.7	922
0.6	0.6	842

necessarily equal to  $k'$  but  $k = k' = 1$  for the pure  $d$  orbitals.  $1-k$  and  $1-k'$  may, therefore, be regarded as a measure of the departure of the actual orbitals from being pure  $d$  orbitals.

Since the orbital reduction factor  $k'$  appears multiplied with the matrix elements of  $L_x$  between states belonging to the  $t_2^4$  and  $t_2^3e$  configuration, for which  $(E_n - E_0)$  in Eq. (3) is very large (see Table I), the calculated susceptibility is not as sensitive to changes in  $k'$  as to changes in  $k$ . The susceptibility was calculated, with parameters of Eq. (1), for a few values of the orbital reduction factors, and the results are given in Table IV. If we take  $k = 0.7$  and  $k' = 0.7$ , the value of susceptibility is  $922 \times 10^{-6}$ . Unfortunately, the experimental values of susceptibility in literature vary from  $860 \times 10^{-6}$  to  $941 \times 10^{-6}$ , and the average value is  $908 \times 10^{-6} \text{ cm}^3 \text{ mole}^{-1}$  (see Ref. 12 for details).

Griffith<sup>15</sup> gave the following analytical expression for the susceptibility of  $t_2^4$ :

$$\chi = 2N\beta^2(k+2)^2(1+\cos\theta)/3m\delta, \quad (4)$$

where  $m = \frac{1}{2}\xi_{nd} + \delta(\sec\theta - 1)$ ,  $2\delta = 15B + 5C + \xi_{nd}$ , and  $\delta \tan\theta = \sqrt{2}\xi_{nd}$ . According to the present calculations the susceptibility from the states belonging to the  $t_2^4$  configuration is  $895 \times 10^{-6}$  and the rest comes from the high-frequency elements. This may be compared with  $1136 \times 10^{-6}$ , given by Eq. (4). The reason for this difference is that in the above formula for  $\chi$ ,  $T_1$  is taken as pure  $t_2^3T_1T_1$ , and  $A_1$  is a combination of  $t_2^4T_1A_1$  and  $t_2^4A_1$ . However, when the states of the  $t_2^3e$  configuration are included, both  $A_1$  and  $T_1$  are diluted by them, and the value of  $\chi$  becomes less than that given by Eq. (4). Also, the value of  $m$ , which is the energy difference between  $t_2^4T_1T_1$  and  $t_2^4T_1A_1$ , is  $2084 \text{ cm}^{-1}$  compared with  $2650 \text{ cm}^{-1}$  calculated in this work, and this reduces the value of  $\chi$  given by Eq. (4).

<sup>1</sup>M. Kotani, J. Phys. Soc. Japan **4**, 293 (1949).

<sup>2</sup>A. D. Liehr and C. J. Ballhausen, Ann. Phys. (N. Y.) **6**, 134 (1959).

<sup>3</sup>J. C. Eisenstein, J. Chem. Phys. **34**, 310 (1961).

<sup>4</sup>J. C. Eisenstein, J. Chem. Phys. **34**, 1628 (1961).

<sup>5</sup>W. A. Runciman and K. A. Schroeder, Proc. Roy. Soc. (London) **A265**, 489 (1962).

<sup>6</sup>K. A. Schroeder, J. Chem. Phys. **37**, 2553 (1962).

<sup>7</sup>R. W. G. Wyckoff, Crystal Structures (Interscience, New York, 1965), Vol. 3.

<sup>8</sup>C. K. Jørgensen, Acta Chem. Scand. **16**, 793 (1962).

<sup>9</sup>C. K. Jørgensen, Mol. Phys. **2**, 309 (1959).

<sup>10</sup>C. K. Jørgensen and J. S. Brinen, Mol. Phys. **5**, 535 (1962).

<sup>11</sup>B. N. Figgis, J. Lewis, R. S. Nyholm, and R. D. Peacock, Discussions Faraday Soc. **26**, 103 (1959).

- <sup>12</sup>R. B. Johannesen and G. A. Candela, *Inorg. Chem.* 2, 67 (1963).
- <sup>13</sup>A. D. Westland and N. C. Bhiwandker, *Can. J. Chem.* 39, 1284 (1961).
- <sup>14</sup>A. Earnshaw, B. N. Figgis, J. Lewis, and R. D. Peacock, *J. Chem. Soc.* 3132 (1961).
- <sup>15</sup>J. S. Griffith, *The Theory of Transition-Metal Ions* (Cambridge U. P., Cambridge, England, 1964).
- <sup>16</sup>Y. Tanabe and H. Kamimura, *J. Phys. Soc. Japan* 13, 394 (1958).